Tunnelling and Underground Space Technology 60 (2016) 121–134

Contents lists available at ScienceDirect

Tunnelling and Underground Space Technology

journal homepage: www.elsevier.com/locate/tust

Model-based airflow controller design for fire ventilation in road tunnels

Šulc Jan [a,b,*], Ferkl Lukáš [b], Cigler Jiří [c], Zápařka Jiří [d]

[a] Czech Technical University in Prague, Faculty of Electrical Engineering, Department of Control Engineering, Karlovo Náměstí 13, 121 35 Prague 2, Czech Republic
[b] Czech Technical University in Prague, University Centre for Energy Efficient Buildings, Třinecká 1024, 273 43 Buštěhrad, Czech Republic
[c] Feramat Cybernetics, s.r.o., Nušlova 2268/1, 158 00 Prague 5, Czech Republic
[d] Satra, s.r.o., Sokolská 32, 120 00 Prague 2, Czech Republic

ARTICLE INFO

Article history:
Received 7 December 2015
Received in revised form 16 July 2016
Accepted 13 August 2016
Available online 26 August 2016

Keywords:
PID
Airflow
Blanka tunnel
Fire ventilation

ABSTRACT

This paper describes a new approach to design the proportional-integral-derivative (PID) controller of the longitudinal airflow velocity in road tunnels for fire situations. Our work shows clearly that the use of a proper model provides valid data for model-based tuning of tunnel controllers, which is demonstrated by real tunnel tests. The design uses the simplified mathematical model of airflow dynamics based on Bernoulli and continuity equations, which describe the airflow dynamics in one dimension. Optimizing controller parameters on site is very time consuming and this problem increases in the case of complex tunnels with several entrance and exit ramps, which typically have occurrences of traffic congestion. Our approach is based on the design of the controller through simulations, which use the mathematical model of airflow velocity in the tunnel. This approach spares a lot of work and time with the controller tuning within tunnel tests. Moreover, it can discover potential problems, which can occur during real instances of fire in the tunnel. The additional advantage of this approach is a possibility to simulate a scenario of errors and failures of some devices, which are important for reliable control of longitudinal airflow velocity. Although this approach is focused primarily on complex road tunnels, due to their complexity and significant time savings with the controller tuning, it can be also used for simpler tunnels with no ramps (usually highway tunnels) where the design of the airflow controller is not as complex compared to the case of road tunnels. This paper also includes a case study of the airflow controller design for the Blanka tunnel complex in Prague, Czech Republic, which is the largest city tunnel in Central Europe.

1. Introduction

After the following series of tragic events in tunnels such as; the Mont Blanc Tunnel – 39 fatalities, the Tauern Road Tunnel – 12 fatalities, the St. Gotthard Tunnel – 11 fatalities and the Gleinalm Tunnel – 5 fatalities, more specific guidances and recommendations for the fire ventilation strategies have been published, e.g. (World Road Association, 2011; CETU, 2003). In summary, reliable control of longitudinal airflow velocity is essential for effective smoke propagation. In the first minutes of a fire event, especially in city tunnels with frequent congestions, it is important to maintain low airflow velocities in the traffic direction to support evacuation. After initial moments of evacuation, conditions for fire-fighters need to be maintained, in order to enable fire-fighting operations. It is achieved through increased longitudinal airflow velocity, in order to push all the smoke downstream of a fire.

In practice, the major parts of industrial processes are controlled by PLC (Parr, 1998). The situation is the same in road tunnels, because ventilation, lighting, drainage and other technological systems are controlled by PLC. The PID controller is the most popular feedback controller in practice, as it is easy for implementation in PLC and, if it is properly tuned, can fulfil most requirements on the control of industrial processes. Moreover, it has a satisfactory response against disturbances and measurement noise. In road tunnels, there can occur several disturbance effects in the case of fire such as; pressure loss caused by fire and device failures (jet fans, sensors).

This paper is divided into six sections, which are structured as follows: In Section 2, the derivation and analysis of the 1D mathematical model of airflow velocity including the modelling of fire

Abbreviations: PID, proportional-integral derivative controller; PLC, programmable logic controller; CFD, Computational Fluid Dynamics; CETU, Centre d'etudes des tunnels; PIARC, Permanent International Association of Road Congresses; CCTV, Closed-circuit television; SIMC, Skogestad Internal Model Control.

* Corresponding author at: Czech Technical University in Prague, Faculty of Electrical Engineering, Department of Control Engineering, Karlovo Náměstí 13, 121 35 Prague 2, Czech Republic.
E-mail address: jan.sulc.2@cvut.cz (Š. Jan).

http://dx.doi.org/10.1016/j.tust.2016.08.006
0886-7798/

dynamics is presented. Section 3 explains the principle of the PID controller for the longitudinal airflow velocity. Section 4 is the case study and gives results from tunnel testing, which took place in the Blanka tunnel complex before opening of the tunnel to traffic. This section also includes a comparison of simulation and real measured data. The final two sections are conclusions and acknowledgements, respectively.

2. Mathematical model of airflow velocity

Our idea is to design the PID controller based on the mathematical model of airflow velocity. The controller performance is influenced by the quality of the mathematical model. For this reason, it is necessary to put significant effort into the development of the airflow dynamics model.

There are two basic approaches to model the airflow dynamics in road tunnels. The first uses the Navier-Stokes equations and the second is based on the Bernoulli and continuity equations. Although the Navier-Stokes equations are non-linear partial differential equations and the airflow dynamics can be described by these equations in three dimensions, they are very computationally time demanding and not suitable for the design of the PID controller.

In recent years, there have been several research groups dealing with the simplified airflow velocity models. One of the most important of them, the research group led by Mizuno, has been dealing with methods of airflow velocity modelling since the 1980s. They have published several important papers, in which they describe the derivation of mathematical models of airflow velocity (Ohashi, 1982; Mizuno, 1991). They verified their approach on two Japanese highway tunnels – the Kan-etsu tunnel (10.965 km) and the Ena-san tunnel (8.625 km). Another group led by a Swede Bring used a similar approach to model the airflow dynamics in one dimension and verified the approach on the real data from the city tunnel in Central Stockholm "Söderledstunneln" in 1997 (Bring et al., 1997). Both mentioned groups were focused on highway tunnels with no entrance and exit ramps. Whereas the Bring's group used the steady-state model of airflow velocity, the Mizuno's group derived the dynamic mathematical model of airflow velocity, which is suitable for a design of the PID controller for airflow velocity. They used the Newton's law of motion for the derivation. In the following, we show the another approach to derive the dynamic mathematical model of airflow velocity through the extended Bernoulli and continuity equation.

2.1. Extended Bernoulli equation for highway tunnel

The Extended Bernoulli equation can be used for the mathematical description of airflow velocity in a tunnel tube. We start with the simplest case of a road tunnel, longitudinally ventilated with uni-directional traffic without any ramps; depicted in Fig. 1.

The Bernoulli equation for an ideal liquid can be written for two points in the tunnel tube as follows (Fox et al., 2011):

$$p_1 - p_2 + \frac{1}{2}\rho(v_1{}^2 - v_2^2) = 0 \tag{1}$$

where p_1, p_2 (Pa) represent the static pressure at two given points in the tunnel tube, v_1, v_2 (m s^{-1}) denote the airflow velocities at two given points of the tunnel tube and ρ (kg m^{-3}) is the air density.

Until now, we have supposed an ideal liquid (air in our case), which is incompressible ($\rho =$ constant) and frictionless and we have also supposed the steady-state airflow ($\frac{\partial v}{\partial t} = 0$). Although the real liquid is compressible, we consider the incompressible flow in the following text, since the assumptions for incompressible flows are valid for Mach numbers considerably lower than 1 (Drikakis and Rider, 2005), which is valid for the airflow velocity in road tunnels where the Mach number does not achieve values higher than 0.03.

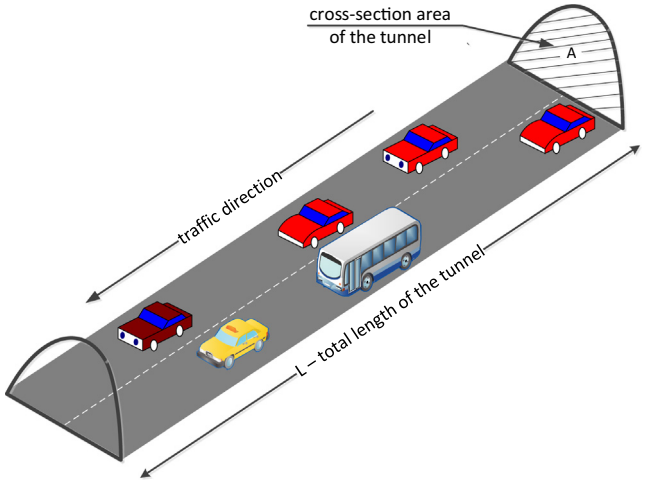

Fig. 1. The most common layout of a road tunnel without ramps.

The Bernoulli equation has to be extended for the real flow and for the design of the airflow velocity controller. If we take air friction, influence of other pressure changes in the tunnel and unsteady flow of air into account, we can extend Eq. (1) in the following way (Fox et al., 2011; White, 2009)

$$p_1 - p_2 + \frac{1}{2}\rho \cdot (v_1{}^2 - v_2^2) - \rho \int_0^{\mathrm{L}} \frac{\partial v(s,t)}{\partial t}\mathrm{d}s + \Delta p(t) = 0 \tag{2}$$

where L (m) is the total length of the tunnel tube, $\rho \int_0^{\mathrm{L}} \frac{\partial v}{\partial t}\mathrm{d}s$ represents the pressure change caused by unsteady flow and Δp (Pa) denotes the total pressure change in the tunnel caused by pressure losses and pressure gains, respectively.

We assume that the airflow velocity along the whole tunnel tube is constant and is only the function of time; $v(s,t) = v(t)$, i.e. $v_1 = v_2$. Furthermore, we assume that the static pressure p_1 is equal to the static pressure p_2, i.e. $p_1 = p_2$, since we consider the same atmospheric conditions such as, temperature and atmospheric pressure, along the whole tunnel. Under these assumptions, Eq. (2) is simplified to

$$-\rho \int_0^{\mathrm{L}} \frac{\partial v(t)}{\partial t}\mathrm{d}s + \Delta p(t) = 0 \tag{3}$$

Since $v(t)$ is only the function of time, Eq. (3) can be simplified after calculating the integral as follows

$$-\rho \mathrm{L}\frac{\mathrm{d}v(t)}{\mathrm{d}t} + \Delta p(t) = 0 \tag{4}$$

The term $\frac{\mathrm{d}v(t)}{\mathrm{d}t}$ is sometimes called local acceleration and is denoted as $a(t)$. The final expression of the Bernoulli equation is following

$$-\rho \mathrm{L}a(t) + \Delta p(t) = 0 \tag{5}$$

In road tunnels, there are many factors, which influence the total pressure change Δp. Pressure losses are usually divided into major losses (air friction) and minor losses (entry of air in the tunnel, air outlet from the tunnel, change of geometry, etc.). All pressure changes, which are taken into account in our mathematical model, can be expressed as

$$\begin{aligned}\Delta p(t) = {} & \Delta p_{fric}(t) + \Delta p_{area}(t) + \Delta p_{fire}(t) + \Delta p_{pist}(t) + \Delta p_{JF}(t) \\ & + \Delta p_{stack}(t) + \Delta p_{wind}(t)\end{aligned} \tag{6}$$

where Δp_{fric} (Pa) denotes the pressure loss caused by air friction, Δp_{area} (Pa) are local area losses, Δp_{fire} (Pa) is the pressure change

caused by occurrence of fire, Δp_{pist} (Pa) denotes influence of vehicles passing through the tunnel, Δp_{JF} (Pa) is the pressure change imposed by running jet fans in the tunnel, Δp_{stack} (Pa) denotes the stack effect and Δp_{wind} (Pa) denotes influence of wind on tunnel portals.

2.1.1. Air friction

Pressure change caused by air friction depends especially on wall roughness and can be computed as (Bring et al., 1997)

$$\Delta p_{fric}(t) = -\frac{1}{2}\rho\lambda(t)\frac{L}{D_h}v(t)|v(t)| \tag{7}$$

where D_h (m) represents the hydraulic diameter of the tunnel, $\lambda(t)$ is the dimensionless coefficient called Darcy friction factor.

The most exact calculation of the friction factor can be performed according to the Colebrook-White equation (Colebrook and White, 1937). Unfortunately, this equation is in the implicit form and cannot be easily used for our purposes. There are several forms to calculate the Darcy friction factor via explicit equations. The most reliable calculation is considered based on the Swamee-Jain equation (Swamee and Jain, 1976)

$$\lambda(t) = \frac{1.325}{\log\left(\frac{\epsilon}{3.7D_h} + \frac{5.74}{Re(t)^{0.9}}\right)^2} \tag{8}$$

where ϵ (m) denotes roughness and Re (–) denotes the Reynolds number. For flow in a pipe or tube, the Reynolds number is generally defined as (Massey and Ward-Smith, 2006)

$$Re(t) = \frac{|v(t)|D_h}{\nu} \tag{9}$$

where ν(m^2 s^{-1}) represents the kinematic viscosity of air.

2.1.2. Local area losses

The term Δp_{area} in Eq. (6) represents pressure losses due to cross-section area changes depending on the cross-section area, shape of transition and direction of airflow. For cases of highway tunnels with no ramps, this pressure loss is composed of several terms

$$\Delta p_{area}(t) = \Delta p_{in}(t) + \Delta p_{out}(t) + \Delta p_{exp}(t) + \Delta p_{con}(t) \tag{10}$$

where Δp_{in} (Pa) is the entrance pressure loss, Δp_{out} (Pa) is the exit pressure loss, Δp_{exp} (Pa) is the pressure loss caused by expansion of the cross-section area and Δp_{con} (Pa) denotes the pressure loss caused by contraction of the cross-section area.

The entrance and exit pressure loss can be calculated according to the following formulas

$$\Delta p_{in}(t) = -\frac{1}{2}\rho\zeta_{in}v(t)^2 \tag{11}$$

$$\Delta p_{out}(t) = -\frac{1}{2}\rho\zeta_{out}v(t)^2 \tag{12}$$

where ζ_{in} (–) and ζ_{out} (–) are entrance and exit loss coefficients, respectively. The entrance and exit loss coefficient for the airflow entering into, respectively exiting from the tunnel, can be determined according to Frost (2006) as $\zeta_{in} = 0.5$ and $\zeta_{out} = 1$.

Two types of shape transition are distinguished in the mathematical model, sudden expansion and sudden contraction; depicted in Figs. 2 and 3, because they are the most occurring transitions in road tunnels. The corresponding pressure losses can be calculated according to the Borda-Carnot equation in the following way (Chanson, 2004; Oertel et al., 2004)

$$\Delta p_{exp}(t) = -\frac{1}{2}\rho\zeta_{exp}v_0(t)^2 = -\frac{1}{2}\rho\left(1 - \frac{A_0}{A_1}\right)^2 v_0(t)^2 \tag{13}$$

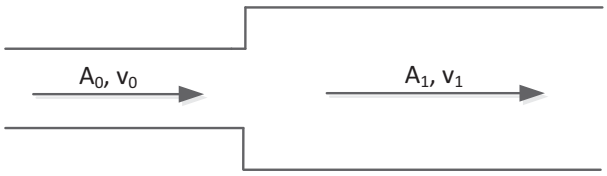

Fig. 2. Sudden expansion of the tunnel cross-section area.

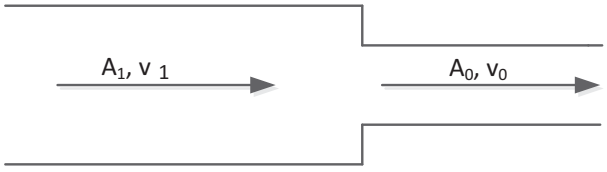

Fig. 3. Sudden contraction of the tunnel cross-section area.

and

$$\Delta p_{con}(t) = -\frac{1}{2}\rho\zeta_{con}v_0(t)^2 = -\frac{1}{2}\rho\left(1 - \frac{A_1}{\beta A_0}\right)^2 v_0(t)^2 \tag{14}$$

where v_1 (m s^{-1}) represents the airflow velocity in the larger cross section area, v_0 (m s^{-1}) represents the airflow velocity in the smaller cross section area, A_1 (m^2) corresponds to the larger cross-section area, A_0 (m^2) corresponds to the smaller cross-section area and β (–) denotes the contraction coefficient, which can be calculated according to Weisbach as follows (Oertel et al., 2004)

$$\beta = 0.63 + 0.37 \cdot \left(\frac{A_0}{A_1}\right)^3 \tag{15}$$

2.1.3. Fire dynamics

In recent years, there have been several research works dealing with the modelling of fire dynamics. Some of them have modelled the fire dynamics using CFD simulations. Vega et al. (2008) developed a numerical 3D simulation of a longitudinal ventilation system in the Memorial tunnel. Wang and Wang (2016) developed a computational model of a tunnel fire for a two-lane highway tunnel. They calculated temperature and critical velocity distribution along the tunnel and compared them with the experimental data from the Memorial tunnel. Vauquelin (2008) created a small-scale tunnel model to study the fire-induced smoke control by the longitudinal and transverse ventilation system. kun Chen et al. (2016) created a reduced-scale single-track railway tunnel to investigate the temperature distribution and behaviour of fires in a tunnel with the natural ventilation. Guo and Zhang (2014) presented an integral theory for a tunnel fire under the longitudinal ventilation. They compared its solution on critical velocity with the experimental data and results of CFD simulation from two different computer programs.

However, results of groups mentioned above cannot be easily used for the one-dimensional model of airflow velocity and for the design of the PID controller. There are several approaches for the modelling of fire dynamics in one dimension. Ingason et al. (2012) simulated and compared data from fire tests in the Runehamar tunnel with the longitudinal ventilation in Norway in 2003. They proposed and compared two methods of calculating the mean temperature of the tunnel fire, which is probably the most difficult part in 1D models of fire dynamics.

According to Vega et al. (2008) and Ingason et al. (2012), the average gas temperature at the location of fire can be calculated as follows:

$$T_f(t) = T_0 + \frac{2}{3}\frac{W(t)}{\rho A C_p |v(t)|} \tag{16}$$

where T_f (K) is the gas temperature at the location of fire, T_0 (K) is the outside temperature of the tunnel, C_p (J kg^{-1}K^{-1}) is the heat capacity of air, W (W) is the heat release rate of the tunnel fire. We assume that the energy transmitted through convection corresponds to 2/3 of the total heat release rate.

Since the gas temperature of the fire is distributed along the whole tunnel, the mean temperature T_m must be chosen for one-dimensional models. The mean temperature T_m is a representative temperature of the region between the fire and downstream exit (nearest exit from the tunnel). Ingason et al. (2012) introduced two methods for the calculation of the mean temperature T_m.

The first method is based on the average temperature at the middle point between the fire source and the downstream exit using the following equation

$$T_m(t) = T_0 + (T_f(t) - T_0) \cdot \exp\left(\frac{cx}{|v(t)|}\right) \tag{17}$$

where T_m (K) is the mean temperature, x(m) is the distance from the fire and we choose $x = L_s$ for the calculation of the mean temperature T_m where L_s (m) is the distance from the fire to the downstream exit and c (s^{-1}) is the constant, which can be calculated as follows

$$c = -\frac{4h_c}{\rho D_h C_p} \tag{18}$$

where h_c(Wm^{-2}K^{-1}) is the convective heat transfer coefficient, which can be calculated using the Petukhov's formula (Petukhov, 1970).

The second method describes the time progress of the mean temperature T_m using the ordinary linear differential equation

$$\frac{\partial T_m(t)}{\partial t} = \frac{|v(t)|}{L_s}(T_f(t) - T_m(t)) - \frac{h_c}{\rho C_p L_s}(T_m(t) - T_0). \tag{19}$$

Eq. (19) can be solved using Runge Kutta method or Euler method with the appropriate time step to preserve stability. For simplification, we use Eq. (17) to calculate the mean temperature in our mathematical model.

When a tunnel fire is being simulated, the pressure change induced by buoyancy forces (smokestack) and expansion of fire must be also taken into account (Pořízek, 2007), i.e.

$$\Delta p_{fire}(t) = \Delta p_{fire,b}(t) + \Delta p_{fire,e}(t) \tag{20}$$

where $\Delta p_{fire,b}$ (Pa) is the pressure change induced by buoyancy forces and $\Delta p_{fire,e}$ (Pa) is the pressure change caused by expansion of fire. Whereas the expansion of fire in 1D models can be neglected, when the system of smoke extraction is in operation, the pressure change governed by buoyancy forces can be neglected only in the case of negligible road gradients (CETU, 2003; Riess et al., 2001).

There are several approaches to calculate the pressure change caused by smokestack in one-dimensioned models. We use the Opstad's model for the calculation of the pressure change in our simulation model (Opstad et al., 1997), since this model can be computed analytically. The model presents limitations in usability only for longitudinally ventilated tunnels without smoke extraction via ventilation machine rooms. Calculation of this pressure change using the Opstad's model can be performed in the following way:

$$\Delta p_{fire,b}(t) = -\frac{|v(t)|g\alpha\rho}{c}\log\left(\frac{T_m(t)}{T_f(t)}\right) \tag{21}$$

where g (m s^{-2}) is the gravitational acceleration, α (–) is the road gradient (negative value corresponds to the declining section).

The following approximate relationship for the calculation of the pressure change caused by expansion of fire in one dimension was determined based on many studies carried out in CETU, which is valid for the longitudinal airflow velocity in the range of 1.5–3.5 m/s (CETU, 2003).

$$\Delta p_{fire,e}(t) = -c_{exp}\frac{W(t)}{v(t)\cdot D_h^2} \tag{22}$$

where c_{exp} is the constant, equals to $9 \cdot 10^{-5}$.

Relationship (22) cannot be used for airflow velocities close to zero, as the pressure change grows to infinity. For this reason, we suggest to approximate the relationship (22) with the following linear equation for airflow velocities lower than 1.5 m/s.

$$\Delta p_{fire,e}(t) = -c_{exp}\frac{W(t)}{v_{min}^2\cdot D_h^2}v(t) \tag{23}$$

where $v_{min} = 1.5$ m s^{-1}.

Eq. (23) preserves continuous transition for airflow velocity equal to 1.5 m/s and set zero value of pressure change for zero airflow velocity.

Since the heat release rate of the tunnel fire $W(t)$ depends on time, Ingason (2009) proposed the curve for the design of a vehicle fire in a road tunnel. This curve describes the heat release rate as an exponential function of time

$$W(t) = W_{max}nr\left(1 - e^{-kt}\right)^{n-1}e^{-kt} \tag{24}$$

where W_{max} (MW) represents the maximum heat release rate during the tunnel fire, r and k are constants, which can be calculated based on the following formulas

$$r = \left(1 - \frac{1}{n}\right)^{1-n} \tag{25}$$

and

$$k = \frac{\ln(n)}{t_{max}} \tag{26}$$

where t_{max} (s) represents the time to reach the maximum heat release rate W_{max}. The only constant, which needs to be chosen arbitrary is n.

Table 1 shows the typical values for fire simulations in road tunnels (Lönnermark, 2005). Two typical fires in road tunnels are taken into account in our simulation model. The first one corresponds to the fire of a passenger car and the other one represents the fire involving a heavy good vehicle (HGV). Depicted in Fig. 4 is the progress of the heat release rate for both considered fires.

2.1.4. Jet fans effect

The pressure change caused by jet fans that run simultaneously at the same place of the tunnel can be expressed as follows (Dally, 1992)

$$\Delta p_{JF}(t) = \eta_{JF}\rho v(t)^2\frac{Q_{JF}(t)}{Q(t)}n_{JF}(t)\left(\frac{v_{JF}(t)}{v(t)} - 1\right) \tag{27}$$

where $Q_{JF}(t)$ (m^3 s^{-1}) is the output airflow of a jet fan, $v_{JF}(t)$ (m s^{-1}) is the average output airflow velocity of a jet fan, $Q(t)$ (m^3 s^{-1}) is the

Table 1
Typical parameters of heat release rate curves for the fire simulation in road tunnels.

Vehicle	Peak HRR (MW)	Average peak HRR (MW)	t_{max} (min)
Passenger car	1.5–8.5	4.1	10–38
2 cars	5.6–10	7.6	13–55
Bus	29–30	29.5	7–8
Heavy good vehicles	13–202	Not identified	8–18

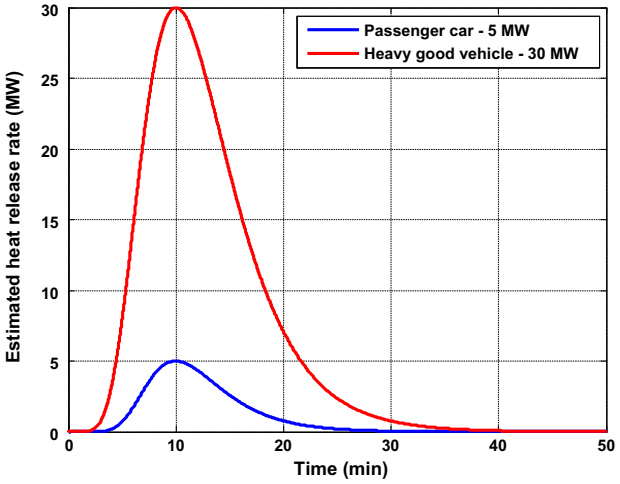

Fig. 4. Typical curves of the heat release rate during fire of a passenger car and a HGV in a road tunnel. Here $n = 16$, $W_{max} = 5$ MW for a passenger car and $n = 10$, $W_{max} = 30$ MW for a HGV. $t_{max} = 10$ min for both passenger car and HGV.

airflow in the tunnel, η_{JF} (–) is the fan efficiency, $n_{JF}(t)$ is the number of jet fans, which run simultaneously in the tunnel and A_{JF} (m^2) is the jet fan outlet area.

For control design purposes, it is preferable to obtain the pressure change that does not depend on v_{JF} and Q. For this reason, we use the following formulas

$$v_{JF}(t) = \frac{Q_{JF}(t)}{A_{JF}} \tag{28}$$

$$Q(t) = v(t)A \tag{29}$$

Substituting Eqs. (28) and (29) into Eq. (27), one obtains the final formula:

$$\Delta p_{JF}(t) = \frac{\eta_{JF}\rho Q_{JF}^2(t)}{A_{JF}A} n_{JF}(t) - \frac{\eta_{JF}\rho Q_{JF}(t)}{A} n_{JF}(t) \cdot v(t) \tag{30}$$

Formulas (27) and (30) holds only for the integer number of running jet fans, i.e. $n_{JF} = \pm 0, 1, 2, \ldots$. For this case, $Q_{JF}(t) = Q_{REF}$ where Q_{REF} is the nominal output airflow of a jet fan. If a jet fan with the variable speed drive is in operation, the following relationship must be taken into account (Dally, 1992)

$$\frac{Q_{JF}(t)}{Q_{REF}} = \frac{\omega_{JF}(t)}{\omega_{REF}} \tag{31}$$

where $\omega_{JF}(t)(\text{min}^{-1})$ is the current speed of a jet fan with the variable speed drive (rotations per minute) and $\omega_{REF}(\text{min}^{-1})$ is the nominal speed of a jet fan (running at maximum speed).

Hence, substituting $Q_{JF}(t)$ from (31) into (30) where $n_{JF} = 1$, one obtains the final relationship for a jet fan with the variable speed drive:

$$\Delta p_{JF}(t) = \frac{\eta_{JF}\rho Q_{REF}^2}{A_{JF}A \cdot \omega_{REF}^2} \omega_{JF}(t)|\omega_{JF}(t)| - \frac{\eta_{JF}\rho Q_{REF}}{A\omega_{REF}} \omega_{JF}(t) \cdot v(t) \tag{32}$$

2.1.5. Piston effect of vehicles

The significant influence, especially in the initial phase of a tunnel fire, can be also caused by vehicles, which are leaving the tunnel and which are blocked upstream of a fire. The pressure change due to the piston effect of vehicles can be calculated based on the following formula (Bring et al., 1997)

$$\Delta p_{pist}(t) = \frac{\rho \sum_i N_i(t) c_{d_i} A_{v_i}}{2A} \cdot (v_{car}(t) - v(t))|v_{car}(t) - v(t)| \tag{33}$$

where $N_i(t)$ (–) is the number of vehicles in the tunnel of the respective type of vehicle, c_{d_i} (–) is the drag coefficient of the respective type of vehicle, A_{v_i} (m^2) is the frontal area of the respective type of vehicle, $v_{car}(t)$ ($m\ s^{-1}$) is the average vehicle velocity in the tunnel.

The mathematical model distinguishes three types of vehicles; passenger cars, vans and heavy good vehicles, but the model can be expanded by the other types of vehicles, such as buses. Table 2 gives the representative values of drag coefficients and frontal areas of the selected types of vehicles (Bring et al., 1997; Wong, 2008; Graebel, 2001).

The absolute value in Eq. (33) captures the situation when the airflow velocity is greater than the average velocity of vehicles and acts as the pressure loss.

We suppose that there is a part of vehicles that drive away from the tunnel and a part of vehicles that is blocked upstream of the fire. Further, we suppose that all entrance portals of the tunnel are closed after the confirmation of fire and no other vehicles come into the tunnel. The piston effect of vehicles leaving the tunnel applies only in the initial phase of fire, since all vehicles gradually leave the tunnel. The number of vehicles behind the fire location as a function of time can be described using the simple equation

$$N_i(t) = \max\left\{0, N_{0,i} \cdot \left(1 - \frac{v_{car}(t)}{L_{leave}} t\right)\right\} \tag{34}$$

where $N_{0,i}$ (–) represents the initial number of vehicles of the respective type behind the location of fire (at the time of the confirmation of fire), L_{leave} (m) denotes the distance to the nearest exit portal of the tunnel (downstream exit) and t (s) represents time of the simulation.

The blocked vehicles cause the pressure loss, as their velocity equals zero, therefore Eq. (33) is reduced to the following form

$$\Delta p_{pist}(t) = -\frac{1}{2}\rho \frac{\sum_{i=1} N_{bl,i} c_{d_{bl,i}} A_{v_{bl,i}}}{A} \cdot v(t)^2 \tag{35}$$

where $N_{bl,i}$ (–) is the number of blocked vehicles of the respective type, $c_{d_{bl,i}}$ (–) is the drag coefficient of blocked vehicles, $A_{v_{bl,i}}$ (m^2) is the average frontal area of blocked vehicles.

2.1.6. Stack effect

The stack effect is caused by the temperature differences between portals of the tunnel. A natural buoyancy exists, therefore the air in the tunnel flows from the place with a higher temperature into the place with a lower temperature. Although there exists a formula for the approximate calculation of the pressure change caused by stack effect, it cannot be simply modelled, because it depends strongly on the current weather conditions at tunnel portals. Moreover, it is practically impossible to measure this effect, because there is usually a lack of sensors (pressure and temperature sensors) inside and outside of the tunnel for the measurement of the stack effect. The approximate calculation of the stack effect can be done based on the following equation (Dally, 1992)

$$\Delta p_{stack}(t) = -\rho g \Delta h \cdot \frac{T_i(t) - T_o(t)}{T_o(t)} \tag{36}$$

where Δh (m) denotes change of altitudes of both tunnel portals, T_i (K) is the average indoor temperature of the tunnel, T_o (K) is the ambient temperature measured near the lower tunnel portal.

Table 2
Representative values of drag coefficients and frontal areas of the selected types of vehicles.

Vehicle	Drag coefficient c_d (–)	Frontal area A_v (m^2)
Passenger cars	0.3–0.5	2–3
Vans	0.4–0.58	7–8.5
HGV	0.74–1.0	7–10

We neglect the pressure change caused by stack effect in our simulation model, because the altitude change of tunnel portals in the case of the Blanka tunnel complex is not significant, thus it causes negligible pressure change compared to the piston effect or air friction. However, the stack effect plays a role of a disturbance in our simulation model, and it can be further used for the robust testing of the designed PID controller for the airflow velocity control, see Section 3.

2.1.7. Influence of wind on tunnel portals

Similarly to the stack effect, it is very difficult to measure and evaluate the wind effect due to inaccurate measurement of wind speed and its direction. The wind speed can achieve sudden fluctuations, which cause fast changes of airflow velocity in the tunnel. Fortunately, road tunnels are usually built to avoid the strong wind effect on tunnel portals thanks to favourable locations against the surrounding terrain. For this reason, we neglect the wind effect on tunnel portals in our mathematical model. However, we are aware that it has a significant influence in the case of highway tunnels, which are usually not situated urban areas.

2.2. Equations for series-parallel network

The mathematical model of airflow velocity differs for tunnels, which have no ramps and are ventilated longitudinally and for tunnels, which have entrance and exit ramps or system of airflow extraction.

The tunnel complex with entrance and exit ramps can be divided into several sections, see Fig. 5 where these sections are determined so that the geometry of these sections is constant, i.e. the cross-section area, slope of the road, hydraulic diameter and number of traffic lanes are constant in these sections. Assuming that airflow velocity in the given tunnel section is constant along the whole section, the parts of the tunnel can be mathematically connected by the continuity equation (Swamee and Sharma, 2008)

$$\sum_i Q_{m_i} = 0 \tag{37}$$

where Q_{m_i} (kg s^{-1}) represents the mass flow rate of air in the respective section.

Suppose that

$$Q_m(t) = \frac{\mathrm{d}m(t)}{\mathrm{d}t} = \rho \frac{\mathrm{d}V(t)}{\mathrm{d}t} = \rho Q_v(t) \tag{38}$$

Assuming that the density of air is constant along the whole section of the tunnel (assumption of incompressibility), the continuity equation is also valid for volumetric flow rates and even for non-stationary (unsteady) flows (Frauenfelder and Huber, 1966), i.e.

$$\sum_i Q_{v_i}(t) = 0 \tag{39}$$

where $Q_{v_i}(t)$ (m^3 s^{-1}) represents the time-dependent volumetric flow rate of air in the respective section. The volumetric flow rate of air in the given tunnel section can be expressed as

$$Q_v(t) = \mathrm{A} \cdot v(t) \tag{40}$$

In fact, Eq. (39) is the equivalent of Kirchhoff's current rule in electrical engineering.

Besides the continuity equation, one has to take Bernoulli equations into account in order to describe fully the dynamics of airflow in the tunnel complex. The algebraic sum of pressure changes in a loop must equal zero (Swamee and Sharma, 2008)

$$\sum_i \Delta p_i(t) - \rho \mathrm{L_i} a_i(t) = 0 \tag{41}$$

where Δp_i (Pa) is the pressure change in the "i-th" tunnel section, $\mathrm{L_i}$ (m) represents the total length of the "i-th" tunnel section and $a_i(t)$ (m s^{-2}) represents the local acceleration of air in the "i-th" tunnel section.

Eq. (41) is the equivalent of Kirchhoff's voltage law where the voltage is the analogous quantity to the pressure change in this case. In the case of tunnels with ramps, the term Δp_{area} has to be expanded by pressure losses caused by dividing and merging flows behind ramps (Idelchick, 2001), which can be generally calculated as follows

$$\Delta p_c(t) = -\frac{1}{2} \rho \zeta_c(t) v_c(t)^2 \tag{42}$$

where Δp_c (Pa) represents the pressure loss caused by merging or dividing flows, $v_c(t)$ (m s^{-1}) denotes the airflow velocity in the "common" section from the airflow direction point of view, i.e. a part upstream of flow division or a part downstream of the flow merging.

Different coefficients ζ_c can be obtained for different cases of dividing and merging flows according to the Idelchik's results (Idelchick, 2001), since his results are considered to be the most plausible for computation. Coefficients ζ_c depend on cross-section areas, directions of flows and volumetric airflow rates in the respective sections.

Any tunnel complex with connected ramps can be described by the combination of continuity equations and Bernoulli equations, as shown on example in Fig. 6.

Example. Fig. 6 represents a road tunnel with one exit ramp where Section 1 represents the tunnel entrance and Sections 2 and 3 represent tunnel exits. This case can be described by the continuity equation as

$$Q_1(t) - Q_2(t) - Q_3(t) = 0 \tag{43}$$

Based on airflow velocities, Eq. (43) can be rewritten in the following way

$$\mathrm{A}_1 v_1(t) - \mathrm{A}_2 v_2(t) - \mathrm{A}_3 v_3(t) = 0 \tag{44}$$

There are two simple loops in the tunnel, shown in Fig. 6, which can be described by the following Bernoulli equations

$$\Delta p_1(t) + \Delta p_2(t) - \mathrm{L}_1 \rho a_1(t) - \mathrm{L}_2 \rho a_2(t) = 0 \tag{45}$$

$$\Delta p_2(t) - \Delta p_3(t) - \mathrm{L}_2 \rho a_2(t) + \mathrm{L}_3 \rho a_3(t) = 0 \tag{46}$$

According to Idelchick (2001), Δp_2 includes also the pressure loss caused by dividing flows

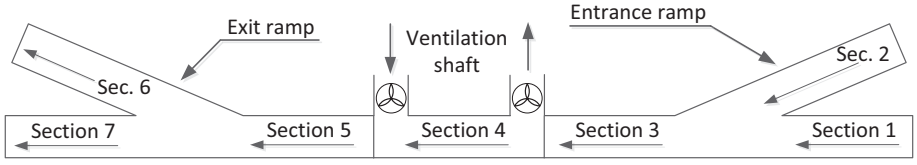

Fig. 5. Schematic representation of a tunnel complex with ramps and with some place for airflow (smoke) extraction and for supply of air, respectively. Arrows denote traffic direction.

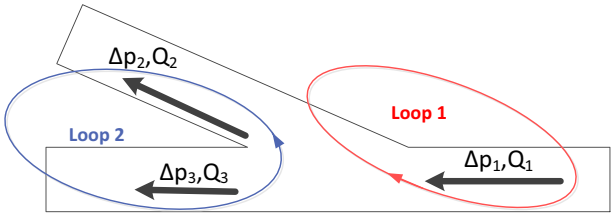

Fig. 6. Schematic representation of an exit ramp including the example of simple loops.

$$\Delta p_{1,2}(t) = -\frac{1}{2}\rho\zeta_{1,2}(t)v_1(t)^2 \tag{47}$$

and Δp_3 includes also the following pressure loss

$$\Delta p_{1,3}(t) = -\frac{1}{2}\rho\zeta_{1,3}(t)v_1(t)^2 \tag{48}$$

2.2.1. Modelling of ventilation machine room dynamics

The case of airflow extraction through a ventilation machine room, shown in Fig. 7, can be described by the continuity equation as well

$$Q_1(t) - Q_2(t) - Q_{vm}(t) = 0 \tag{49}$$

where $Q_1(t), Q_2(t)$ are volumetric airflow rates in the respective tunnel section, $Q_{vm}(t)$ is the volumetric airflow rate through ventilation machine room.

The volumetric airflow rate through a ventilation machine room is time dependent and can be modelled as the first order dynamic system

$$\frac{dQ_{vm}(t)}{dt} = a_q Q_{vm}(t) - a_q Q_{max} \tag{50}$$

where Q_{max} ($m^3\ s^{-1}$) is the maximum (steady-state value) of the volumetric airflow rate through the ventilation machine room, a_q is the constant, which influences the dynamic characteristics of the volumetric airflow rate through the ventilation machine room such as rise time, etc.

These constants can be approximately estimated from the catalogue data and from the real process of starting fans in the ventilation machine room, eventually.

2.3. Derivation of state space description

The state space description of the mathematical model of airflow velocity in a tunnel must be derived for the design of the airflow velocity controller. The state space description allows to simulate the progress of airflow velocity depending on time in all considered tunnel sections taking running jet fans, airflow extraction through ventilation machine rooms and various input conditions (influence of piston effect of vehicles, parameters of fire in the tunnel, initial airflow velocity in the tunnel, etc.) into account.

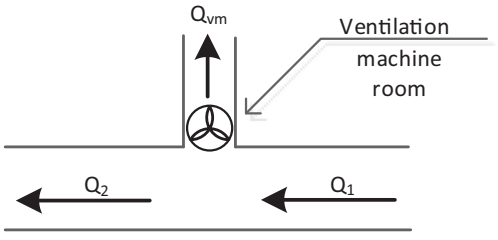

Fig. 7. Schematic representation of airflow extraction from the tunnel through ventilation machine room.

The state space description can be generally expressed in the following form

$$\dot{\mathbf{v}}(t) = f(\mathbf{v}(t), \mathbf{u}(t)) \tag{51}$$

where $\dot{\mathbf{v}}(t)$ represents the vector of time derivatives of airflow velocities $\left(\frac{dv(t)}{dt}\right)$ in all tunnel sections, $\mathbf{v}(t)$ represents the vector of airflow velocities in all tunnel sections, $\mathbf{u}(t)$ represents the vector of control inputs, which is composed of the number of running jet fans in the respective tunnel section and volumetric airflow rates through the respective ventilation machine rooms and f is the non-linear vector field depending on airflow velocities in the respective tunnel sections and control inputs.

We have found an approach to obtain the state space description in the form (51) for a general highway tunnel or tunnel complex with ramps or with a system of airflow (smoke) extraction, too.

Example. We show the derivation of the state space description on the example of a road tunnel, shown in Fig. 6 where there is depicted a road tunnel with only one exit ramp. As stated above, we have obtained the set of three non-linear differential-algebraic Eqs. (44)–(46) where the unknown variables are airflow velocities $v_1(t), v_2(t), v_3(t)$.

If we express time derivatives of airflow velocities $\dot{v}(t)$ in Eq. (44), we obtain (together with the remaining equations) the following set of equations

$$\begin{aligned} &A_1\dot{v}_1(t) - A_2\dot{v}_2(t) - A_3\dot{v}_3(t) = 0 \\ &\Delta p_1(t) + \Delta p_2(t) - L_1\rho\dot{v}_1(t) - L_2\rho\dot{v}_2(t) = 0 \\ &\Delta p_2(t) - \Delta p_3(t) - L_2\rho\dot{v}_2(t) + L_3\rho\dot{v}_3(t) = 0 \end{aligned} \tag{52}$$

After modifying the set of Eqs. (52), one obtains

$$\begin{aligned} &A_1\dot{v}_1(t) - A_2\dot{v}_2(t) - A_3\dot{v}_3(t) = 0 \\ &-L_1\rho\dot{v}_1(t) - L_2\rho\dot{v}_2(t) = -\Delta p_1(t) - \Delta p_2(t) \\ &-L_2\rho\dot{v}_2(t) + L_3\rho\dot{v}_3(t) = -\Delta p_2(t) + \Delta p_3(t) \end{aligned} \tag{53}$$

The set of linear Eqs. (53) can be solved analytically where the unknown variables are time derivatives of airflow velocities $\dot{v}_i$.

Generally, the set of Eqs. (53) can be rewritten into the following matrix form

$$\mathbf{A}\dot{\mathbf{v}}(t) = \mathbf{b}(t)(\mathbf{v}(t), \mathbf{u}(t)) \tag{54}$$

where $\mathbf{A}$ is the $n \times n$ square matrix with the known coefficients and n is the number of sections of the tunnel, $\mathbf{b}$ is the $n \times 1$ vector formed by Δp_i, which depends on the individual airflow velocities v_i and control inputs u_i.

For our example, the matrices $\mathbf{A}$ and $\mathbf{b}$ have the following form:

$$\mathbf{A} = \begin{pmatrix} A_1 & -A_2 & -A_3 \\ -L_1\rho & -L_2\rho & 0 \\ 0 & -L_2\rho & L_3\rho \end{pmatrix} \tag{55}$$

$$\mathbf{b}(t) = \begin{pmatrix} 0 \\ -\Delta p_1(t) - \Delta p_2(t) \\ -\Delta p_2(t) + \Delta p_3(t) \end{pmatrix} \tag{56}$$

Once the state space description of the airflow dynamics in a road tunnel is obtained, the time simulation of airflow velocity can be performed through the numerical methods for a solution of the set of non-linear differential equations (e.g. Euler method or Runge-Kutta methods Cellier and Kofman, 2006). These methods require explicit expression of time derivatives of airflow velocities in the individual tunnel sections. These derivatives can be calculated in every time step by solving the set of linear algebraic Eq. (54).

3. Control of longitudinal airflow velocity

3.1. Control requirements on longitudinal airflow velocity

In 1999 the organization PIARC published a report (Piarc Technical Commitee on Tunnel Operations, 1999), which identifies a lack of specific rules and standards for fire ventilation control. For this reason, several national authorities published guidelines (Espinosa et al., 2010), which involve several standards for fire ventilation control in city tunnels: Austria (RVS 09.03.31), Germany (RABT) (Richtlinien für die Ausstattung und den Betrieb von Strassentunnel, 2006), France (Circulaire Interministrielle 20–63 dated 20th August 2000) (Instruction technique annexe a la Circulaire 2000-63,) or Switzerland (FEDRO) (Ventilation of Road Tunnels, 1999). The stated guidelines have one common aspect; the distinction between the evacuation phase and fire-fighting phase.

Our approach for the design of airflow velocity controller is focused primarily on complex road tunnels with ramps (usually city tunnels) where there is a potential risk of congestion or stop and go situation and two phases of fire ventilation are recommended. The aim is to control the longitudinal airflow velocity upstream of a fire via jet fans in the tunnel.

3.1.1. Evacuation phase

In the first moments of a fire, the target of fire ventilation is to provide conditions for self-evacuation without any assistance of emergency services. The low longitudinal airflow velocity, around 1.2 m/s, is ideal for the smoke propagation in the stratified way, i.e. the smoke propagates in both directions (upstream and downstream of fire) under the ceiling in the separate layer from the fresh air layer. It enables people to escape the tunnel through emergency exits.

3.1.2. Fire-fighting phase

After several minutes, the fire builds up and the smoke starts to fill the whole cross-section area of the tunnel and the second phase of fire ventilation needs to be activated. The aim is to increase the longitudinal airflow velocity in order to push the smoke only downstream of a fire. The minimum longitudinal airflow velocity to prevent smoke propagation upstream of fire is called the critical velocity (Li et al., 2010). The critical velocity depends on many factors, such as heat release rate, cross-section area, slope of the road and its value can be determined from CFD simulations. Its value is usually 2.2–3.5 m/s (Sturm et al., 2015).

3.1.3. Unaffected tunnel

Besides the requirements for airflow velocity control in the fire-affected tunnel, a fixed plan is normally also defined for the ventilation of the unaffected tunnel. The goal is to ensure that the unaffected tunnel is at a higher pressure than the affected tunnel, in order to prevent smoke propagation from the affected tunnel to the unaffected tunnel through emergency exits or tunnel portals. The desired longitudinal airflow velocity in the unaffected tunnel should be negative (against the direction of traffic), say −1 or −1.5 m/s.

For the cases 3.1.1, 3.1.2 and 3.1.3, there should be implemented three controllers of the longitudinal airflow velocity.

- Controller for the first phase (evacuation phase) in the fire-affected tunnel,
- Controller for the second phase (fire-fighting phase) in the fire-affected tunnel,
- Controller in the unaffected tunnel.

3.2. Principle of the PID controller

The important assumption for the use of the PID controller is a measurement of the physical quantity to be controlled. In the case of fire ventilation, the controlled quantity is the airflow velocity upstream of the fire location and airflow velocity in the unaffected tunnel tube. The discrete-time PID controller is used for the control of airflow velocity (Aström and Haegglund, 1995)

$$u(t) = \mathrm{K_p} e(t) + \mathrm{K_i} \sum_{i=0}^{t} e(i)\Delta\mathrm{T} + \mathrm{K_d} \frac{e(t) - e(t-1)}{\Delta\mathrm{T}} \tag{57}$$

where $e(t)$ can be calculated as follows

$$e(t) = v_{ref}(t) - v(t) \tag{58}$$

and $\mathrm{K_p}$ is the proportional constant of the controller, $\mathrm{K_i}$ is the integral constant of the controller, $\mathrm{K_d}$ is the derivative constant of the controller $e(t), e(t-1)$ is the control error in the certain time t, or $t-1$ respectively (error between the set-point value and the currently measured value of the airflow velocity), $v_{ref}(t)$ is the set-point value of the airflow velocity upstream of the fire location at the certain time t, $v(t)$ is the currently measured value of the airflow velocity upstream of the fire location at the time $t, \Delta\mathrm{T}$ (s) is the sample period of the controller, $u(t)$ represents the output of the PID controller (manipulated variable), the number of jet fans, located upstream of the fire location, which are to be run.

For each control problem (first phase, second phase and unaffected tunnel), the priority of jet fans is specified. The manipulated variable $u(t)$ has to be distributed among the individual admissible jet fans according to the priority of jet fans. The jet fans located upstream of the fire location are prioritized before the jet fans located behind and jet fans with the variable speed drives are prioritized before jet fans equipped with soft-starters, due to the possibility of continuous speed control.

Example. The manipulated variable in the fire-affected tunnel, calculated according to Eq. (57), is $u(t) = 3.4$ at the certain time t. Jet fans 1, 2, 3, 4 and 5 are admissible. Jet fans 1, 2, 3 are located upstream of the fire incident, thereby these jet fans should be used at first. Whereas jet fan 1 is equipped with the variable speed drive, which allows the continuous regulation of speed, jet fans 2, 3, 4 and 5 do not enable the continuous regulation. The only regulation possibility of these jet fans is in the way of on/off switching. The algorithm distributes the manipulated variable $u(t)$ as follows

- 0.4 falls to jet fan 1 with the variable speed drive, located upstream of the fire location, i.e. it runs at 40% of nominal speed,
- 2 fall to jet fans 2 and 3, located upstream of the fire location, i.e. they run at the nominal (100%) speed,
- 1 falls to jet fan 4, located downstream of the fire location.

In the case of jet fan failure, the jet fan that is out of service, can be easily substituted by the next jet fan in the priority list.

Once the fire alarm in the particular fire section is confirmed, some of jet fans have to be blocked. It is prohibited to start jet fans, which are located directly in the fire section, because it could support and expand fire. Each fire section has a priority list with the specific sequence of jet fans, which are admissible for the control. However, there can be fire sections in the tunnel, which do not have any jet fans equipped with the variable speed drive, which means that the continuous regulation of speed is not possible in this case. In this case, one has two possibilities how to deal with the fractional part of the manipulated variable $u(t)$, either to neglect it or to round it.

The algorithm must further take technical limitations of jet fans into account, especially the minimum speed of jet fans equipped with the variable speed drive or maximum admissible starts per hour of jet fans equipped with soft-starters due to the effective engine cooling.

3.3. Design and simulation of PID controller

Once the mathematical model of airflow velocity in a road tunnel is created, one can design the PID controller using this mathematical model. The design can be performed in several steps:

1. Preliminary design of the PID controller using standard methods, e.g. Root locus (Franklin et al., 2010), SIMC (Skogestad, 2003) or Ziegler-Nichols (Ziegler et al., 1942),
2. Tuning of the controller using simulations,
3. Robustness testing of the controller against disturbance signals and measurement noise, e.g. start-up of ventilation machine rooms, piston effect of vehicles, stack effect, fire pressure loss,
4. Post-tuning of the controller for the real operation during the examinations in the tunnel.

Performance of the controller can be verified through simulation tools like *Matlab/Simulink*. For the simulation, we use the feedback control scheme with the PID controller, which is shown in Fig. 8. There are two different subsystems in the control loop; the PID controller and the mathematical model of airflow velocity. Current output from the mathematical model (longitudinal airflow velocity) is fed through feedback to the input of the PID controller. The PID controller calculates the manipulated variable, based on Eq. (57) and provides it into the mathematical model.

We performed numerous simulations, in which we tested different numerical methods for the solution of non-linear differential equations and the Euler integration method with the fixed time-step 1 s seems to be the best choice for the simulation of airflow dynamics with respect to the stability and computational time of the simulation. Our findings are in accordance with the project (Euler-Rolle et al., 2016) where no stability issues or excessive errors arose by using an adequately short step size 0.5 s or 1 s.

The aim of the paper is not the exact description of the controller tuning, but rather a demonstration how to create and use the mathematical model of a road tunnel for the design of the airflow velocity controller. For this reason, we do not show how we tuned the constants of the PID controller in the following part of the paper. However, we assume that the SIMC method (Skogestad, 2003) is probably the simplest method for the design of the PID controller, especially suitable in cases where the model of the process dynamics is known.

4. Case study: the Blanka tunnel complex

4.1. Basic information

The Blanka tunnel complex is one of the largest underground structures in the Czech Republic with the total length of more than 5 km. The tunnel was open to traffic in September 2015 and the traffic intensity in the tunnel is usually more than 60,000 vehicles per day. It is composed of two tunnel tubes with uni-directional traffic and forms the north-west part of the Prague City Ring Road, see Fig. 9. Besides two main portals Malovanka and Troja, there are exit and entry ramps from each tube at two locations called Prašný most and U Vorlíků that divide the tunnel complex into three tunnels (Databank of the company Satra, spol. s r. o.).

- Brusnice, three-lane tunnel, total length 1.4 km, predominantly cut and cover tunnel and partially driven tunnel,
- Dejvice, two-lane tunnel, total length 1.0 km, fully cut and cover tunnel,
- Bubeneč, two-lane tunnel, total length 3.09 km, predominantly driven tunnel, partially cut and cover tunnel.

4.2. Safety concept of the tunnel complex

Besides the high traffic intensity with often congested traffic situations, there are together 15 exit and entry portals, which complicate the smoke control regarding the rescue tube. Another aspect for fire safety design is the longitudinal slope of −5% (declining tube) in the Bubeneč tunnel where buoyancy of fire pushes the smoke upstream. All these aspects led to requirements for quick fire detection system and reliable longitudinal airflow velocity control.

4.3. Fire detection system

Besides the quick detection of fire, it is also very important to localize a fire place correctly. The standard requirement for tunnels in the Czech Republic is a linear heat detector. The linear heat detector is a proprietary cable, which detects heat conditions and occurred fire along the whole tunnel. In general, linear heat detectors are reliable, but with disadvantage of slower detection depending on the longitudinal airflow velocity. After good experience in St. Gotthard tunnel, the detection system in the Blanka tunnel complex is based on smoke detectors. Smoke detectors work on the principle of continuous monitoring of smoke concentration. There are 125 smoke detectors in the tunnel, defining 125 detection sections, where the fire can be localized. The linear heat detector is divided according to these 80–90 m long sections. The Blanka

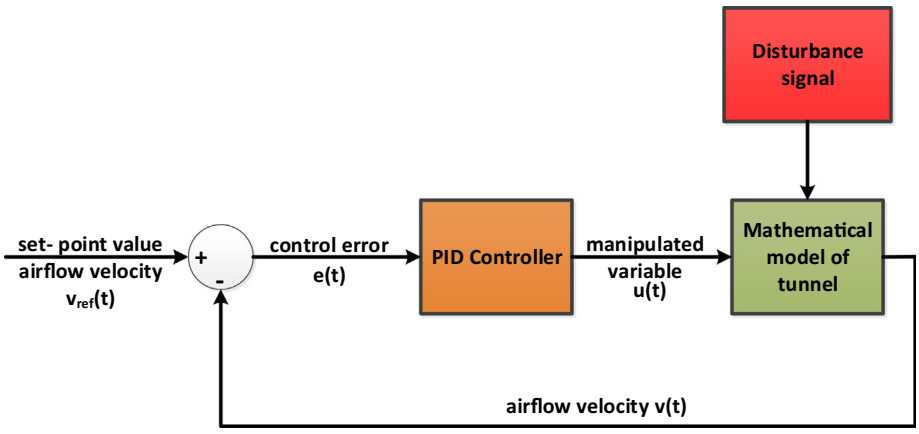

Fig. 8. The control loop used for simulation of airflow velocity control.

Fig. 9. An aerial map of the Blanka tunnel complex in Prague, Czech Republic. The tunnel forms the north-west part of the Prague City Ring Road (Satra, spol. s r. o. [online], 2012).

tunnel complex is equipped with the camera system (CCTV) for traffic supervision. CCTV uses real-time video processing algorithms to identify smoke in images. It can analyse changes such as brightness or contrast, therefore it is able to evaluate burning vehicle. Moreover, it helps the operator to evaluate status during traffic accidents. The camera system in the Blanka tunnel complex involves 180 cameras.

4.4. Fire ventilation

The PID controller controls the airflow velocity in the evacuation phase and fire-fighting phase in the fire-affected tunnel. Moreover, there is also the PID controller for the control of the airflow velocity in the unaffected tunnel. Parameters of the PID controllers differ for different detection sections. Each detection section has the following parameters:

1. Proportional constant of all controllers (first phase, second phase and controller in the unaffected tunnel),
2. Integral constant of all controllers,
3. Derivative constant of all controllers,
4. Priority list of jet fans, which can be used for the control of airflow velocity,
5. Set-point values for all controllers.

Table 3 gives the general overview of set-point values used for different controllers mentioned above.

There are no strict requirements on airflow velocity control. However, the set-point (required) value of airflow velocity should be achieved as fast as possible, say, in a few minutes. The airflow velocity should be maintained in the desired band of, say ±0.3 m/s from the set-point value, larger oscillations of the airflow velocity should be suppressed as fast as possible and reversal of flow at the blocked vehicles is strictly prohibited.

Table 3
Set-point values of airflow velocity for different phases of fire ventilation in the Blanka tunnel complex. Negative value of airflow velocity denotes opposite direction of flow to traffic.

Phase	Set-point value (m/s)
First phase (evacuation phase) in the fire-affected tunnel	0.9–1.6
Second phase (fire-fighting phase) in the fire-affected tunnel	1.9–3.6
Unaffected tunnel	−1.5

Together with airflow velocity control, there is also a system of the smoke extraction. In driven parts with the highest longitudinal slope of 5%, the smoke extraction is distributed through several openings, which are located at the ceiling of the tunnel at regular intervals 80 m. The hot smoke from a burning vehicle rises to the ceiling, passes through openings and then under the road into the fire duct. The remotely controlled dampers are located in the fire duct and must be opened in the case of fire. The smoke is pushed through the fire duct and finally extracted from the tunnel through axial fans in a ventilation machine room to the outside environment. In the first (evacuation) phase, the smoke is extracted through two openings (one upstream and one downstream of fire), see Fig. 11, and the extracted amount of air is approximately 160 m^3/s. In the second (fire-fighting) phase, the extracted amount of air is 240–320 m^3/s and smoke is extracted through 3–4 openings (according to two- or three-lane tunnel) located downstream of fire, see Fig. 12.

Unfortunately, it was not possible to use this distributed system of smoke extraction along the whole tunnel complex because of technical limitations in the cut and cover tunnel Dejvice. In this case, the smoke is extracted through one point in the tunnel, massive point extraction.

Fig. 10. Axial fans in the ventilation machine room Letná (Databank of the company Satra, spol. s r. o.).

In case of fire in portal sections (located near to the exit portals and ramps), the smoke is removed from the tunnel through portals, and thus ventilation machine rooms are not in operation for this case.

For longitudinal airflow velocity control, there are 88 jet fans (in total in both tubes) installed, located under the ceiling of the tunnel. The major part of jet fans is controlled by soft-starters with on/off regulation, however, there is at least one jet fan with the variable speed drive in each ventilation section of the tunnel, which offers continuous regulation of speed. There are 27 airflow velocity sensors calibrated at the mean airflow velocity, which provide a feedback for the PID controllers.

Smoke extraction is provided by 30 axial flow fans in 5 ventilation machine rooms; Troja, Letná, Prašný most, Špejchar and Střešovice; see Fig. 10. Ventilation machine rooms are constructed separately for both, northern and southern tunnel, i.e. they do not share the same axial fans and ventilation shafts.

The axial fans in ventilation machine rooms have variable speed drives for the control of extracted amount of air, which is used for normal operation. However, during fire, the axial fans are operated at the constant pre-set value without any continuous regulation. The ventilation machine rooms Prašný most and Špejchar are intended for the massive point extraction.

4.5. Simulation of airflow velocity control

The mathematical model of airflow dynamics in the Blanka tunnel complex was created according to the procedure described in Section 2. The schematic representation of the Blanka tunnel complex is shown in Fig. 13. The overall dynamic system is represented by 34 unknown variables, airflow velocities in the individual tunnel sections (marked as v 1–34 in the scheme). Since there is no binding between the northern and southern tunnel, the

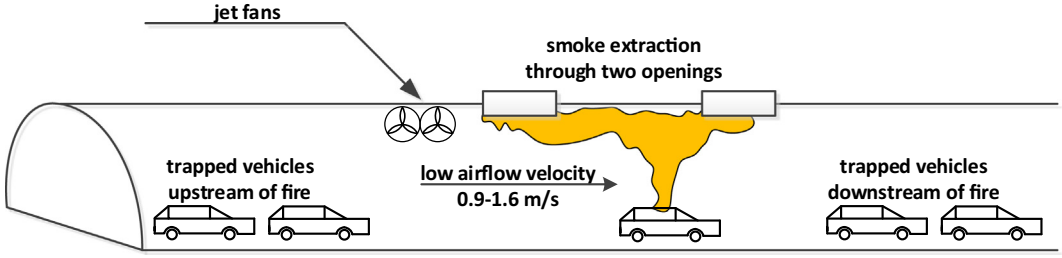

Fig. 11. Distributed smoke extraction in the first (evacuation) phase of fire ventilation in driven tunnel sections. PID controller controls the airflow velocity upstream of fire.

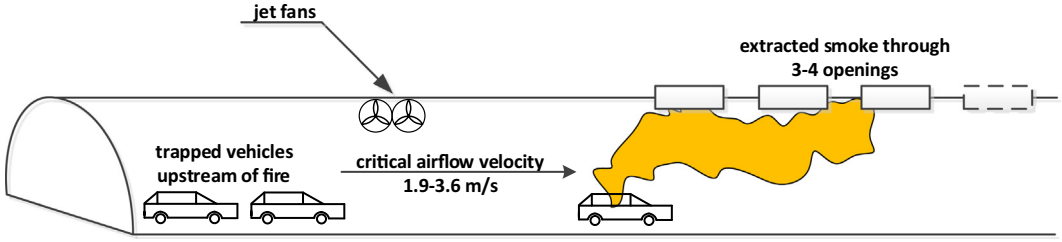

Fig. 12. Distributed smoke extraction in the second (fire-fighting) phase of fire ventilation in driven tunnel sections. PID controller controls the airflow velocity upstream of fire.

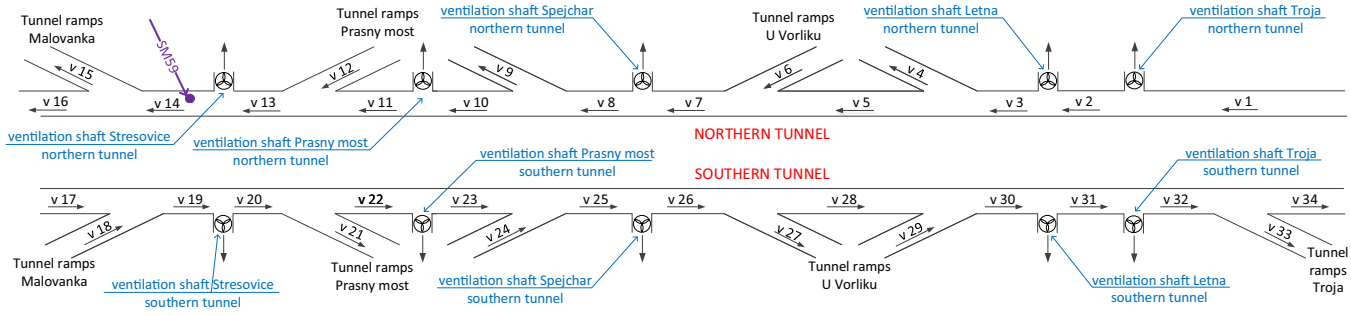

Fig. 13. Schematic illustration of the Blanka tunnel complex including all tunnel ramps, ventilation machine rooms (shafts) and airflow velocities in the individual tunnel sections.

mathematical model can be calculated separately for both tubes in order to accelerate the computational time.

We show the simulation of airflow velocity control in detection section SM59, which is located in the northern tunnel section Brusnice. The approximate location of section SM59 is depicted in Fig. 13. Since section SM59 is a portal section, located near to the exit ramp Malovanka, ventilation machine rooms for smoke extraction are not in operation in this case. Three different scenarios are simulated for section SM59:

1. Airflow velocity control in the fire-affected tunnel without any disturbance,
2. Airflow velocity control in the fire-affected tunnel including disturbance caused by smokestack and expansion of fire. The fire is represented by the burning passenger car (5 MW) in this case,
3. The same as the point 2, however the fire is represented by a heavy good vehicle (30 MW).

The input parameters of fire, see Eq. (21)–(23), which are used for the simulation are given in Table 4. The simulation considers the same curves of HRR as in Fig. 4. Other important parameters of the simulation are stated in Table 5.

The simulation demonstrates the robustness of the designed PID controller against disturbances. The simulation covers only the first phase of fire ventilation, since it is crucial for successful evacuation.

During the tunnel testing, we determined that the derivative action does not have a significant influence on the control performance. Moreover, it requires filtering of the airflow velocity signal due to the measurement noise. For this reason, the K_d constant is set to zero and only the PI controller is in operation.

Simulation results of the airflow velocity control using the PI controller in the fire-affected tunnel are depicted in Fig. 14. The upper graph represents the airflow velocity upstream of fire and the bottom graph represents the control output (manipulated variable), number of jet fans, which are to be run. There are three lines in the graphs representing different simulation scenarios. Whereas the blue one (scenario 1) does not consider any disturbance effect, the red one (scenario 2) represents the fire of a passenger car (5 MW) and the green one (scenario 3) represents the fire of a heavy good vehicle (30 MW). The black dashed line is the desired band of airflow velocity upstream of the fire source that corresponds to 1.6 ± 0.3 m/s. The road gradient equals 2.8%, therefore the smoke propagates due to the smokestack downstream of fire (in the traffic direction) towards the exit portal Malovanka. The pressure change caused by smokestack increases the airflow velocity in the fire-affected section of the tunnel.

As the blue line is not influenced by the disturbance caused by fire, the control performance is best among all simulated scenarios.

Table 4
Simulation parameters of fire for the considered scenarios.

Parameter	Scenario 1	Scenario 2	Scenario 3
n (–)	–	16	10
t_{max} (min)	–	10	10
W_{max} (MW)	–	5	30
T_0 (K)	–	283	283

Table 5
Parameters of section SM59, which are taken into account in the simulation.

Parameter	Value
D_h (m)	8.7
A (m^2)	84
α (–)	0.028
L_s (m)	355

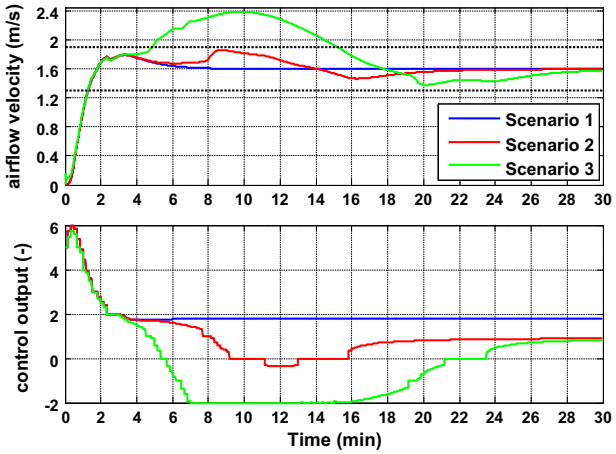

Fig. 14. Simulation of the airflow velocity control in detection section SM59 during the first phase of fire ventilation. Constants of the PID controller are set as follows: $K_p = 3, K_i = 0.03, K_d = 0$ and the sample time of the controller is $\Delta T = 10$ s.

The airflow velocity achieves set-point value in 2 min and is kept in the desired band during the whole simulation. The control performance in scenario 2 is also satisfactory, since the airflow velocity is kept in the desired band as well. As can be seen, the control output is negative in the 10th minute of simulation (heat release rate of fire achieved maximum), which corresponds to the reverse operation of jet fans that brake the airflow velocity.

The control performance for scenario 2 is better than the case of scenario 3. As can be seen, in case of scenario 3, the airflow velocity is not kept in the desired band during 5–15 min after the start of the simulation. Note that fire of 30 MW causes a major disturbance for the PI controller, however, the control output saturates at the value −2, i.e. jet fans brake the airflow velocity as much as possible, therefore the disturbance is suppressed as fast as possible and the control performance is acceptable.

4.5.1. Comparison with real data

Finally, we show the comparison of simulation and real measurement of airflow velocity in section SM59, which was performed during the tunnel testing. The pressure change caused by fire is not considered in the simulation, since the control performance was tested without using a real fire in the tunnel.

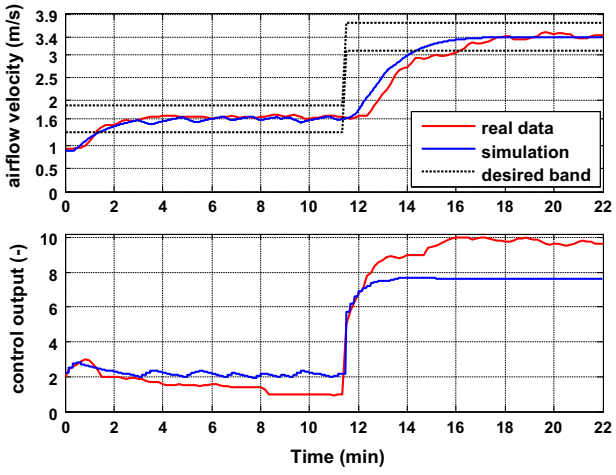

Fig. 15. Comparison of real measurement and simulation of airflow velocity control in section SM59. Constants of the PID controller are set as follows: $K_p = 3, K_i = 0.03, K_d = 0$ in the first phase and $K_p = 2, K_i = 0.03, K_d = 0$ in the second phase of fire ventilation. The sample time of the controller is $\Delta T = 10$ s.

The result of the airflow velocity control is shown in Fig. 15 where the measured airflow velocity is represented by the red line in the upper graph. For the comparison, the blue line represents the modelled airflow velocity. The bottom graph shows the number of activated jet fans, control output of the PI controller. Both phases of fire ventilation were tested, while the second phase started approximately after 11 min from the beginning of the test. The set-point value is set to 1.6 m/s in the first phase and 3.4 m/s in the second phase of fire ventilation.

As can be seen, the set-point value of airflow velocity was achieved in 3 min and the airflow velocity was kept in the desired band of 1.6 ± 0.3 m/s till the end of the first phase. The second phase of fire ventilation started after 11 min, while the desired band of airflow velocity was increased to 3.4 ± 0.3 m/s. As can be seen, the PI controller increased the number of running jet fans in the second phase, the set-point value was achieved in 5 min and the airflow velocity was kept in the desired band.

Simulation and real measurement of airflow velocity show relatively good correspondence with respect to the way of modelling where the 1D model of airflow velocity is crated only based on physical laws and measured data from the tunnel are not used for the modelling of airflow dynamics.

5. Conclusion

The paper presents a new approach for the design of airflow velocity control using PID controllers. The approach uses the simplified mathematical model of airflow velocity based on continuity equations and Bernoulli equations. The mathematical model is verified through simulations, which are compared with the measured airflow velocity during the system testing in the Blanka tunnel complex, situated in Prague, Czech Republic.

Although there are some errors between measured and modelled airflow velocity, the mathematical model in the tunnel is suitable for the design of the airflow velocity control, especially for complex road tunnels where there are a lot of sections with different airflow dynamics. This approach can significantly spare time with controller tuning, because it allows tuning of controllers through the simulation model. The controller can be post-tuned during the system testing in the tunnel. Thanks to this approach, it is possible to test unexpected situations (e.g. jet fan failure) and disturbances (e.g. pressure change caused by piston effect of vehicles leaving the tunnel or pressure change caused by fire effect), which can occur during the real fire situations in the tunnel.

The mathematical model of airflow velocity in the tunnel can be further used for the design of the operational ventilation control, i.e. for the maintenance of the indoor environmental quality (concentrations of exhaust gases and opacity).

Acknowledgements

This work has been supported by the project of University Centre for Energy Efficient Buildings of the Czech Technical University in Prague and further through the internal grant of the CTU SGS16/232/OHK3/3T/13. Significant thanks belong to the ventilation designer Jan Pořízek from the company Satra, s.r.o. for his valuable advice and comments, which contributed to the final version of this paper.

References

Aström, K.J., Haegglund, T., 1995. PID Controllers: Theory, Design and Tuning. Instrument Society of America.
Bring, A., Malmström, T., Boman, C., 1997. Simulation and measurement of road tunnel ventilation. Tunn. Undergr. Space Technol. 12 (3), 417–424.
Cellier, F.E., Kofman, E., 2006. Continuous System Simulation. Springer.
CETU, November 2003. Dossier pilote des tunnels quipements. Section 4.1, Ventilation.
Chanson, H., 2004. The Hydraulics of Open Channel Flow: An Introduction, second ed. Elsevier Butterworth-Heinemann.
Colebrook, C.F., White, C.M., 1937. Experiments with fluid friction in roughened pipes. R. Soc. London Proc. Ser. A 161, 367–381.
Dally, B., 1992. Practical Guide to Fan Engineering. Pitman Publishing Limited, Colchester.
Drikakis, D., Rider, W., 2005. High-Resolution Methods for Incompressible and Low-Speed Flows. Springer.
Espinosa, I., Fernández, S., Del Rey, I., Alarcón, E., 2010. Experiences on the specification of algorithms for fire and smoke control in road tunnels. In: Proceedings of the 5th International Conference Tunnel Safety and Ventilation in Graz, pp. 39–43.
Euler-Rolle, N., Bammer, C., Reinwald, M., Jakubek, S., 2016. Model based dynamic feedforward control of longitudinal tunnel ventilation. In: Proceedings of the 8th International Conference 'Tunnel Safety and Ventilation', Graz, pp. 212–219.
Fox, R., McDonald's, A.T., Pritchard, P.J., 2011. Introduction to Fluid Mechanics, eighth ed. John Willey & Sons.
Franklin, G.F., Powell, D.J., Emani-Naemi, A., 2010. Feedback Control of Dynamic Systems, sixth ed. Pearson Education.
Frauenfelder, P., Huber, P., 1966. Introduction to Physics: Mechanics, Hydrodynamics, Thermodynamics. Pergamon.
Frost, W.H., 2006. Minor loss coefficients for storm drain modeling with swmm. J. Water Manage. Model., 517–546
Graebel, W.P., 2001. Engineering Fluid Mechanics. Taylor & Francis, 29 West 35th Street New York, NY 100001.
Guo, X., Zhang, Q., 2014. Analytical solution, experimental data and CFD simulation for longitudinal tunnel fire ventilation. Tunn. Undergr. Space Technol. 42, 307–313. http://dx.doi.org/10.1016/j.tust.2014.03.011 <http://www.sciencedirect.com/science/article/pii/S0886779814000467>.
Idelchick, I., 2001. Handbook of Hydraulic Resistance, third ed. Begell House.
Ingason, H., 2009. Design fire curves for tunnels. Fire Safety J. 44 (2), 259–265.
Ingason, H., Lönnermark, A., Li, Y.Z., 2012. Model of ventilation flows during large tunnel fires. Tunn. Undergr. Space Technol. 30, 64–73. http://dx.doi.org/10.1016/j.tust.2012.02.007 <http://www.sciencedirect.com/science/article/pii/S0886779812000399>.
Instruction technique annexe a la Circulaire 2000-63, 2000. CETU, Tech. Rep., CETU, Bron, France.
Kun Chen, C., Xiang Zhu, C., Ya Liu, X., Kang, H., Wei Zeng, J., Yang, J., 2016. The effect of fuel area size on behavior of fires in a reduced-scale single-track railway tunnel. Tunn. Undergr. Space Technol. 52, 127–137. http://dx.doi.org/10.1016/j.tust.2015.12.002 <http://www.sciencedirect.com/science/article/pii/S088677981530331X>.
Li, Y.Z., Lei, B., Ingason, H., 2010. Study of critical velocity and backlayering length in longitudinally ventilated tunnel fires. Fire Safety J. 45 (68), 361–370.
Lönnermark, A., 2005. On the Characteristics of Fires in Tunnels Ph.D. Thesis. Department of Fire Safety Engineering, Lund Institute of Technology, Lund University, September.
Massey, B., Ward-Smith, J., 2006. Mechanics of Fluids, eighth ed. Taylor&Francis.
Mizuno, A., 1991. An optimal control with disturbance estimation for the emergency ventilation of a longitudinally ventilated road tunnel. In: Flucome '91:Proceedings of the 3rd Triennial International Symposium on Fluid Control, Measurement, and Visualization. American Society of Mechanical Engineers, pp. 393–399.
Oertel, H., Prandtl, L., Böhle, M., Mayes, K., 2004. Prandtl's Essentials of Fluid Mechanics, second ed. Springer.
Ohashi, H., 1982. A new ventilation method for the kanetsu road tunnel. In: Proc. 4th international symposium on the aerodynamics and ventilation of vehicle tunnels (York, U.K. March 23–25, 1982). BHRA Fluid Engineering Centre, Cranfield, UK, pp. 31–47.
Opstad, K., Aune, P., Henning, J.E., 1997. Fire emergency ventilation capacity for road tunnels with considerable slope. In: Proceedings of the 9th International Symposium on Aerodynamics and Ventilation of Vehicle Tunnels, Aosta, pp. 535–543.
Parr, E.A., 1998. Industrial Control Handbook. Industrial Press Inc.
Petukhov, B., 1970. Heat transfer and friction in turbulent pipe flow with variable properties. Adv. Heat Transfer 6, 504–506.
Piarc Technical Commitee on Tunnel Operations, 1999. Fire and Smoke Control In Road Tunnels, Tech. rep., PIARC.
Pořízek, J., 2007. Fire Test in Mrázovka Tunnel. Tunel 16 (3), 40–44.
Richtlinien für die Ausstattung und den Betrieb von Strassentunnel, 2006. RABT, Tech. Rep., Forschungsgesellschaft für das Strassen und Verkehrswesen, Germany.
Riess, I., Bettelini, M., Brandt, R., 2001. Smoke extraction in tunnels with considerable slope. In: Proceedings of the 4th International Conference Safety in Road and Rail Tunnels.
Satra, spol. s r. o., Data Archives of the Company.
Skogestad, S., 2003. Simple analytic rules for model reduction and PID controller tuning. J. Process Control 13, 291–309. http://dx.doi.org/10.1016/S0959-1524(02)00062-8.
Satra, spol. s r. o. [online], Tunelový komplex Blanka (in Czech), [cit. 2012-10-12]. Available on <http://www.tunelblanka.cz>.
Sturm, P., Beyer, M., Rafiei, M., 2015. On the problem of ventilation control in case of a tunnel fire event. Case Stud. Fire Safety http://dx.doi.org/10.1016/j.csfs.2015.11.001.

Swamee, P., Jain, A., 1976. Explicit equations for pipe-flow problems. J. Hydraul. Div., 657–664
Swamee, P.K., Sharma, A.K., 2008. Design of Water Supply Pipe Networks. John Wiley & Sons.
Vauquelin, O., 2008. Experimental simulations of fire-induced smoke control in tunnels using an airhelium reduced scale model: principle, limitations, results and future. Tunn. Undergr. Space Technol. 23 (2), 171–178. http://dx.doi.org/10.1016/j.tust.2007.04.003 <http://www.sciencedirect.com/science/article/pii/S0886779807000454>.
Vega, M.G., Díaz, K.M.A., Oro, J.M.F., Tajadura, R.B., Morros, C.S., 2008. Numerical 3d simulation of a longitudinal ventilation system: memorial tunnel case. Tunn. Undergr. Space Technol. 23 (5), 539–551. http://dx.doi.org/10.1016/j.tust.2007.10.001 <http://www.sciencedirect.com/science/article/pii/S0886779807001010>.
Ventilation of Road Tunnels, 1999. FEDRO, Tech. Rep., FEDRO, Switzerland.
Wang, F., Wang, M., 2016. A computational study on effects of fire location on smoke movement in a road tunnel. Tunn. Undergr. Space Technol. 51, 405–413. http://dx.doi.org/10.1016/j.tust.2015.09.008 <http://www.sciencedirect.com/science/article/pii/S0886779815301103>.
White, F.M., 2009. Fluid Mechanics, seventh ed. Mc Graw-Hill, New York.
Wong, J.Y., 2008. Theory of Ground Vehicles, fourth ed. John Wiley & Sons.
World Road Association (PIARC), 2011. Road Tunnels Manual.
Ziegler, J.G., Nichols, N.B., Rochester, N.Y., 1942. Optimum settings for automatic controllers. Trans. ASME, 759–765.